

# Pathological Basis for Deficient Excitatory Drive to Cortical Parvalbumin Interneurons in Schizophrenia

Daniel W. Chung, M.S., Kenneth N. Fish, Ph.D., David A. Lewis, M.D.

**Objective:** Deficient excitatory drive to parvalbumin-containing cortical interneurons is proposed as a key neural substrate for altered gamma oscillations and cognitive dysfunction in schizophrenia. However, a pathological entity producing such a deficit has not been identified. The authors tested the hypothesis that cortical parvalbumin interneurons receive fewer excitatory synaptic inputs in individuals with schizophrenia.

**Method:** Fluorescent immunohistochemistry, confocal microscopy, and post-image processing techniques were used to quantify the number of putative excitatory synapses (i.e., the overlap of vesicular glutamate transporter 1-positive [VGlut1+] puncta and postsynaptic density protein 95-positive [PSD95+] puncta) per surface area of parvalbumin-positive (PV+) or calretinin-positive (CR+) neurons in the dorsolateral prefrontal cortex from schizophrenia subjects and matched unaffected comparison subjects.

**Results:** Mean density of VGlut1+/PSD95+ puncta on PV+ neurons was 18% lower in schizophrenia, a significant

difference. This deficit was not influenced by methodological confounds or schizophrenia-associated comorbid factors, not present in monkeys chronically exposed to antipsychotic medications, and not present in CR+ neurons. Mean density of VGlut1+/PSD95+ puncta on PV+ neurons predicted the activity-dependent expression levels of parvalbumin and glutamic acid decarboxylase 67 (GAD67) in schizophrenia subjects but not comparison subjects.

**Conclusions:** To the authors' knowledge, this is the first demonstration that excitatory synapse density is lower selectively on parvalbumin interneurons in schizophrenia and predicts the activity-dependent down-regulation of parvalbumin and GAD67. Because the activity of parvalbumin interneurons is required for generation of cortical gamma oscillations and working memory function, these findings reveal a novel pathological substrate for cortical dysfunction and cognitive deficits in schizophrenia.

*Am J Psychiatry* 2016; 173:1131–1139; doi:10.1176/appi.ajp.2016.16010025

Cognitive dysfunction is a core and clinically critical feature of schizophrenia (1) but responds poorly to available medications (2). Therefore, identifying the neural substrate for these cognitive deficits is critical for the development of new therapeutic interventions. Certain cognitive deficits, such as impaired working memory, appear to emerge from altered gamma oscillations in the dorsolateral prefrontal cortex (DLPFC) (3). Because cortical gamma oscillations require the activity of parvalbumin-containing (PV) interneurons (4, 5), deficient cortical PV interneuron activity could provide the neural substrate for altered prefrontal gamma oscillations and consequently impaired working memory in schizophrenia.

Lower glutamatergic drive to PV interneurons has been hypothesized to be the cause of deficient PV interneuron activity in schizophrenia (6–8). This hypothesis is based on findings that experimental manipulations in model systems that reduce glutamatergic drive to PV interneurons result in lower PV interneuron activity accompanied by lower expression of activity-dependent gene products (e.g., PV and the GABA-synthesizing enzyme glutamic acid decarboxylase

67 [GAD67]), abnormal gamma oscillations, and working memory deficits (9–12). Consistent with this hypothesis, postmortem studies have repeatedly shown lower PV and GAD67 levels in the DLPFC of schizophrenia subjects (13–17), which are thought to reflect lower glutamatergic drive to a subset of PV neurons and not a loss of PV neurons in the illness (13, 15, 18, 19). These deficits do not seem to be due to a global reduction in excitatory drive to all interneuron subtypes, as calretinin-containing (CR) interneurons, the most abundant interneuron subtype in the primate DLPFC (20), appear to be relatively unaffected in schizophrenia (15, 16, 21). However, the pathological basis for lower glutamatergic drive selectively onto PV interneurons, such as fewer excitatory synapses on these neurons, has not been identified in people with schizophrenia.

Therefore, in this study, we used multilabeling fluorescent immunohistochemistry, confocal imaging, and a custom post-image processing method to directly assess excitatory synapses on parvalbumin-positive (PV+) neurons in the DLPFC from matched pairs of schizophrenia and unaffected comparison

**TABLE 1. Summary Characteristics of Study Subjects**

Characteristic	Unaffected Comparison Subjects		Schizophrenia Subjects	
	N	%	N	%
Sex				
Male	15	75	15	75
Female	5	25	5	25
Race				
White	16	80	14	70
Black	4	20	6	30
	Mean	SD	Mean	SD
Age (years) <sup>a</sup>	46.3	12.1	45.2	11.8
Postmortem interval (hours) <sup>b</sup>	16.4	5.5	15.4	6.3
Tissue storage time (months) <sup>c</sup>	110.8	33.9	103.5	28.3

<sup>a</sup> Nonsignificant difference between groups (paired t test:  $t=1.3$ ,  $df=19$ ,  $p=0.21$ ).

<sup>b</sup> Nonsignificant difference between groups (paired t test:  $t=0.7$ ,  $df=19$ ,  $p=0.47$ ).

<sup>c</sup> Nonsignificant difference between groups (paired t test:  $t=0.9$ ,  $df=19$ ,  $p=0.36$ ).

subjects. We tested the hypotheses that 1) lower PV levels in subjects with schizophrenia reflect altered PV expression per neuron and not a loss of PV+ neurons, 2) PV+, but not calretinin-positive (CR+), neurons receive fewer excitatory synaptic inputs in subjects with schizophrenia, and 3) fewer excitatory synapses on PV+ neurons are associated with activity-dependent down-regulation of PV and GAD67 levels.

## METHOD

### Human Subjects

Brain specimens ( $N=40$ ) were obtained during routine autopsies conducted at the Allegheny County Office of the Medical Examiner (Pittsburgh) after consent was obtained from the next of kin. An independent team of clinicians made consensus DSM-IV diagnoses for each subject based on structured interviews with family members and review of medical records. The absence of a psychiatric diagnosis was confirmed in unaffected comparison subjects using the same approach. All procedures were approved by the University of Pittsburgh Committee for the Oversight of Research and Clinical Training Involving the Dead and the Institutional Review Board for Biomedical Research. The subjects were selected based on a postmortem interval less than 24 hours in order to avoid the effect of postmortem interval on protein immunoreactivity (see the “Supplementary Methods” section in the data supplement accompanying the online version of the article). In addition, to control for the autofluorescence emitted by lipofuscin, which accumulates with aging (22), all subjects were less than 62 years of age. To control for experimental variance and to reduce biological variance, each subject with schizophrenia or schizoaffective disorder ( $N=20$ ) was paired with one unaffected comparison subject for sex and as closely as possible for age (see Table S1 in the online data supplement). The mean age, postmortem interval,

and tissue storage time did not differ between subject groups (Table 1).

### Fluorescent Immunohistochemistry

Paraformaldehyde-fixed coronal tissue sections ( $40\ \mu\text{m}$ ) containing DLPFC area 9 were processed for fluorescent immunohistochemistry as previously described (23). Sections were pretreated for antigen retrieval (0.01 M sodium citrate for 75 minutes at  $80^\circ\text{C}$ ) and then incubated for 72 hours in the following primary antibodies: PV (mouse, 1:1000; Swant, Bellinzona, Switzerland), CR (goat, 1:1000; Swant), postsynaptic density protein 95 (PSD95; rabbit, 1:250; Cell Signaling, Danvers, Mass.), and vesicular glutamate transporter 1 (VGLut1; guinea pig, 1:250; Millipore, Billerica, Mass.). Tissue sections were then incubated for 24 hours with secondary antibodies (donkey) conjugated to Alexa 488 (antimouse, 1:500), 568 (antirabbit, 1:500), 647 (anti-guinea pig, 1:500) (all from Invitrogen, Carlsbad, Calif.) or biotin (antigoat, 1:200; Fitzgerald, Acton, Mass.). Sections were then incubated with streptavidin 405 (1:200; Invitrogen) for 24 hours. After washing, the sections were mounted in the Prolong Gold Antifade reagent (Life Technologies, Carlsbad, Calif.), coded to obscure diagnosis and subject number, and stored at  $4^\circ\text{C}$  until imaging. All antibodies used in this study have been previously shown to specifically recognize the targeted protein (see “Supplementary Methods” in the online data supplement).

### Image Acquisition

Images were acquired on an Olympus (Center Valley, Pa.) IX81 inverted microscope equipped with an Olympus spinning disk confocal unit, a Hamamatsu EM-CCD digital camera (Bridgewater, N.J.), and a high-precision BioPrecision2 XYZ motorized stage with linear XYZ encoders (Ludl Electronic Products, Hawthorne, N.J.) using a  $60\times 1.40$  NA SC oil immersion objective. Ten image stacks ( $512\times 512$  pixels;  $0.25\ \mu\text{m}$  z-step) in layer 2 or 4 from each section were selected using a previously published method for systematic random sampling (24). Layer 2 or 4 was defined as 10%–20% or 50%–60% of the pia-to-white matter distance, respectively (25). We sampled these two layers as layer 4 contains a high density of PV interneurons (20) and prominently lower PV mRNA levels in schizophrenia (15, 21), whereas layer 2 contains a high density of CR interneurons (26). The very low densities of PV interneurons in layer 2 and of CR interneurons in layer 4 precluded the sampling of these neurons. Lipofuscin for each stack was imaged using a custom fifth channel (excitation wavelength: 405 nm; emission wavelength: 647 nm) at a constant exposure time as previously described (27).

### Post-Image Processing and Object Sampling

Each fluorescent channel was deconvolved using the algorithm for blind deconvolution in Autoquant (Media Cybernetics, Rockville, Md.) to improve resolving power. VGLut1+ and PSD95+ puncta were used to identify the pre- and postsynaptic elements, respectively, as these molecular

markers have been previously used to define excitatory synapses in PV interneurons (11, 28, 29). Masking of VGlut1+ and PSD95+ puncta was performed using the previously described method (30) (see “Supplementary Methods” and Figure S1 in the online data supplement). Edges of PV+ or CR+ cell bodies were segmented by the MATLAB edge function using the Canny edge detector operator (31). The edges of segmented objects were closed, filled, and size-gated ( $>80 \mu\text{m}^3$ ) to limit the boundaries of PV+ or CR+ cell bodies. All PV+ and CR+ cell body masks were manually cleaned for final analyses (see Figure S1 in data supplement). We sampled objects that localized within the middle 80% of z-planes ( $\sim 32 \mu\text{m}$ ), based on antibody penetration efficiency analyses to avoid edge effects (see “Supplementary Methods” in online data supplement). The mean volume of tissue sampled did not differ between subject groups (layer 2:  $t=0.3$ ,  $df=19$ ,  $p=0.78$ ; layer 4:  $t=0.03$ ,  $df=19$ ,  $p=1.00$ ). The mean numbers of VGlut1+ puncta and PSD95+ puncta sampled in layer 2 or layer 4 did not differ between subject groups (in all cases,  $t < |1.6|$ ,  $df=19$ ,  $p > 0.12$ ), indicating the absence of any group differences in cortical lamination. Numbers of VGlut1+/PSD95+ puncta per surface area of PV+ or CR+ cell bodies were calculated in order to determine the density of excitatory synapses on PV+ or CR+ neurons.

### Antipsychotic-Exposed Monkeys

Male monkeys (*Macaca fascicularis*) received oral doses of haloperidol (12–14 mg), olanzapine (5.5–6.6 mg), or placebo (N=6 per each group) twice daily for 17–27 months as previously described (32). Trough plasma levels for haloperidol and olanzapine were within the range associated with clinical efficacy in humans (32). The monkeys were euthanized in triads (one monkey from each of the three groups) on the same day. Coronal sections (40  $\mu\text{m}$ ) containing DLPFC area 9 from each monkey were processed for fluorescent immunohistochemistry as described above.

### Statistics

Two analysis of covariance (ANCOVA) models were used to assess the main effect of diagnosis on the dependent measures. The paired ANCOVA model included subject pair as a blocking factor and postmortem interval and tissue storage time as covariates. This paired model accounts both for our attempts to balance diagnostic groups for sex and age and for the parallel tissue processing of both subjects in a pair, but it is not a true statistical paired design. Therefore, we also used an unpaired ANCOVA model that included sex, age, postmortem interval, and storage time as covariates. Most covariates were not significant and therefore were not included in the final analyses; exceptions included an effect of tissue storage time on the mean density of PSD95+ puncta on PV+ cell bodies ( $F=5.5$ ,  $df=1, 35$ ,  $p=0.03$ ) by unpaired ANCOVA and an effect of storage time on the mean surface area of CR+ cell bodies ( $F=6.5$ ,  $df=1, 18$ ,  $p=0.03$ ) and on the mean density of VGlut1+/PSD95+ puncta on CR+ cell bodies ( $F=8.8$ ,  $df=1, 18$ ,  $p=0.008$ ) by paired ANCOVA.

The potential influence of comorbid factors (e.g., diagnosis of schizoaffective disorder; history of substance dependence or abuse; nicotine, antidepressant, benzodiazepine, and/or sodium valproate use at time of death; death by suicide) in the schizophrenia subjects was assessed by an ANCOVA model with each factor as the main effect and sex, age, postmortem interval, and storage time as covariates. Pearson’s correlation analysis was performed to assess the relationship of the density of VGlut1+/PSD95+ puncta on PV+ cell bodies to somal PV immunoreactivity levels or to PV and GAD67 mRNA levels obtained from previously published studies (33, 34). For the antipsychotic-exposed monkeys, an ANCOVA was used to assess the main effect of antipsychotic treatment on the dependent measures with triad as a blocking factor.

## RESULTS

### Lower PV Levels in PV Interneurons in Schizophrenia

We sampled PV+ neurons in DLPFC layer 4 (Figures 1A and 1B), as lower PV mRNA levels in schizophrenia are prominent in this layer (15, 21). Consistent with those findings, mean PV protein levels in PV+ cell bodies were 34% lower in subjects with schizophrenia, a significant difference (Figure 1C). The mean numbers of PV+ neurons in identical volumes of sampled tissue did not differ between subject groups (Figure 1D). Finally, we observed a left shift in the frequency distribution of PV levels per PV+ cell body in schizophrenia subjects relative to comparison subjects (Figure 1E). Together, these findings suggest that lower PV levels in schizophrenia reflect lower PV expression in a subset of PV neurons and not a deficit in PV neuron number.

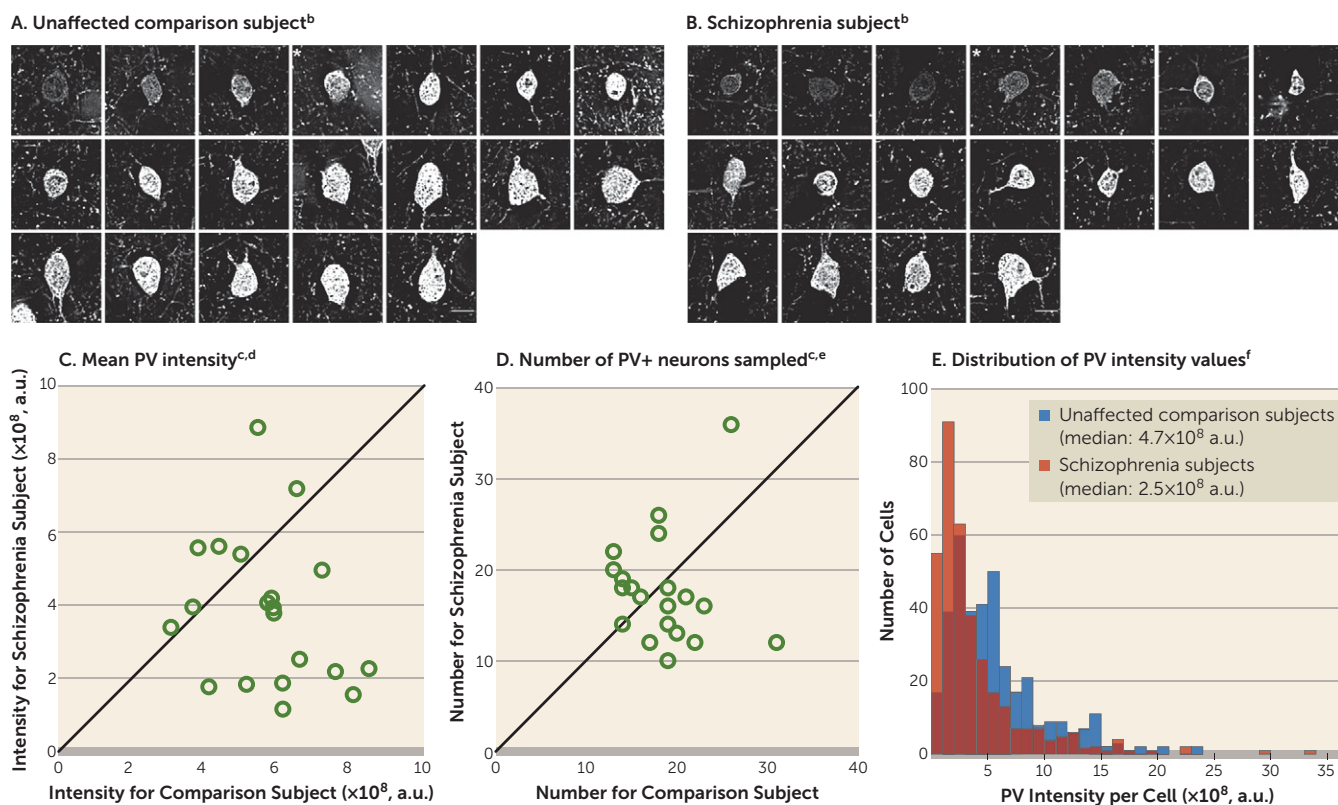
### Fewer Excitatory Synaptic Inputs to PV Interneurons in Schizophrenia

The pre- and postsynaptic elements of excitatory synapses on PV+ neurons were identified by VGlut1+ puncta and PSD95+ puncta, respectively (Figures 2A and 2B). Excitatory synapses were defined by the overlap of VGlut1+ and PSD95+ (VGlut1+/PSD95+) puncta. The mean density of VGlut1+/PSD95+ puncta on PV+ cell bodies was 18% lower in schizophrenia subjects, a significant difference (Figure 2C). The mean densities of VGlut1+ and PSD95+ puncta on PV+ cell bodies were also significantly lower—12% and 19%, respectively—in the schizophrenia subjects (Figures 2D and 2E), reflecting fewer pre- and postsynaptic glutamatergic structures on PV+ neurons.

### Lack of Effect From Methodological Confounds or Disease-Associated Comorbid Factors

The mean surface area of PV+ cell bodies did not differ between subject groups (Figure 2F), indicating that the lower density of excitatory synapses on PV+ neurons in schizophrenia is not due to a larger surface area of PV+ cell bodies. The mean VGlut1 and PSD95 protein levels in labeled puncta on PV+ cell bodies did not differ between subject groups (see Figure S2 in the online data supplement), suggesting that our findings of fewer synaptic

**FIGURE 1. Sampling of PV+ Neurons and Quantification of PV Immunoreactivity Levels in Dorsolateral Prefrontal Cortex Area 9 for Each Matched Pair of Unaffected Comparison and Schizophrenia Subjects<sup>a</sup>**



<sup>a</sup> a.u., arbitrary units.

<sup>b</sup> Panels A and B illustrate the representative sampling of PV+ neurons with varying range of PV intensity levels from one subject pair (Hu1543 and Hu10026; see Table S1 in the data supplement accompanying the online version of this article). Images show a z-plane that contains the largest surface area of PV+ cell body. \* denotes PV+ neurons shown in Figure 2. Scale bars=10 μm.

<sup>c</sup> In panels C and D, the scatterplots indicate the levels of dependent measures (indicated in the heading of each graph) for each unaffected comparison and schizophrenia subject in a pair (open circles). Data points below the diagonal unity line indicate a lower level in the schizophrenia subject relative to the matched unaffected comparison subject.

<sup>d</sup> The mean somal PV immunoreactivity level in PV+ cell bodies was 34% lower in the schizophrenia subjects than in the unaffected comparison subjects (schizophrenia: mean=3.8×10<sup>8</sup>, SD=2.0×10<sup>8</sup>; comparison: mean=5.7×10<sup>8</sup>, SD=1.5×10<sup>8</sup>). The difference was statistically significant (paired: F=9.7, df=1, 19, p=0.006; unpaired: F=11.3, df=1, 36, p=0.002).

<sup>e</sup> The mean number of PV+ neurons sampled (schizophrenia: mean=17.7, SD=6.0; comparison: mean=18.5, SD=4.6) was 4% lower in the schizophrenia subjects but did not differ significantly between groups (paired: F=0.2, df=1, 19, p=0.65; unpaired: F=0.3, df=1, 36, p=0.59).

<sup>f</sup> Panel E illustrates the frequency distributions of somal PV intensity values of PV+ neurons sampled from schizophrenia subjects and unaffected comparison subjects. Each bin represents 1×10<sup>8</sup> a.u.

structures in schizophrenia were not biased by lower levels of synaptic markers. Finally, the mean density of VGlut1+/PSD95+ puncta on PV+ cell bodies did not differ among schizophrenia subjects as a function of assessed comorbid factors (see Figure S3 in the data supplement) and was not altered in monkeys chronically exposed to antipsychotic medications (see Figure S4D in data supplement). Together, these findings suggest that fewer excitatory synapses on PV+ neurons reflect the disease process of schizophrenia and are not due to methodological confounds or other factors commonly associated with the illness.

### Unaffected Excitatory Synaptic Inputs to CR Interneurons in Schizophrenia

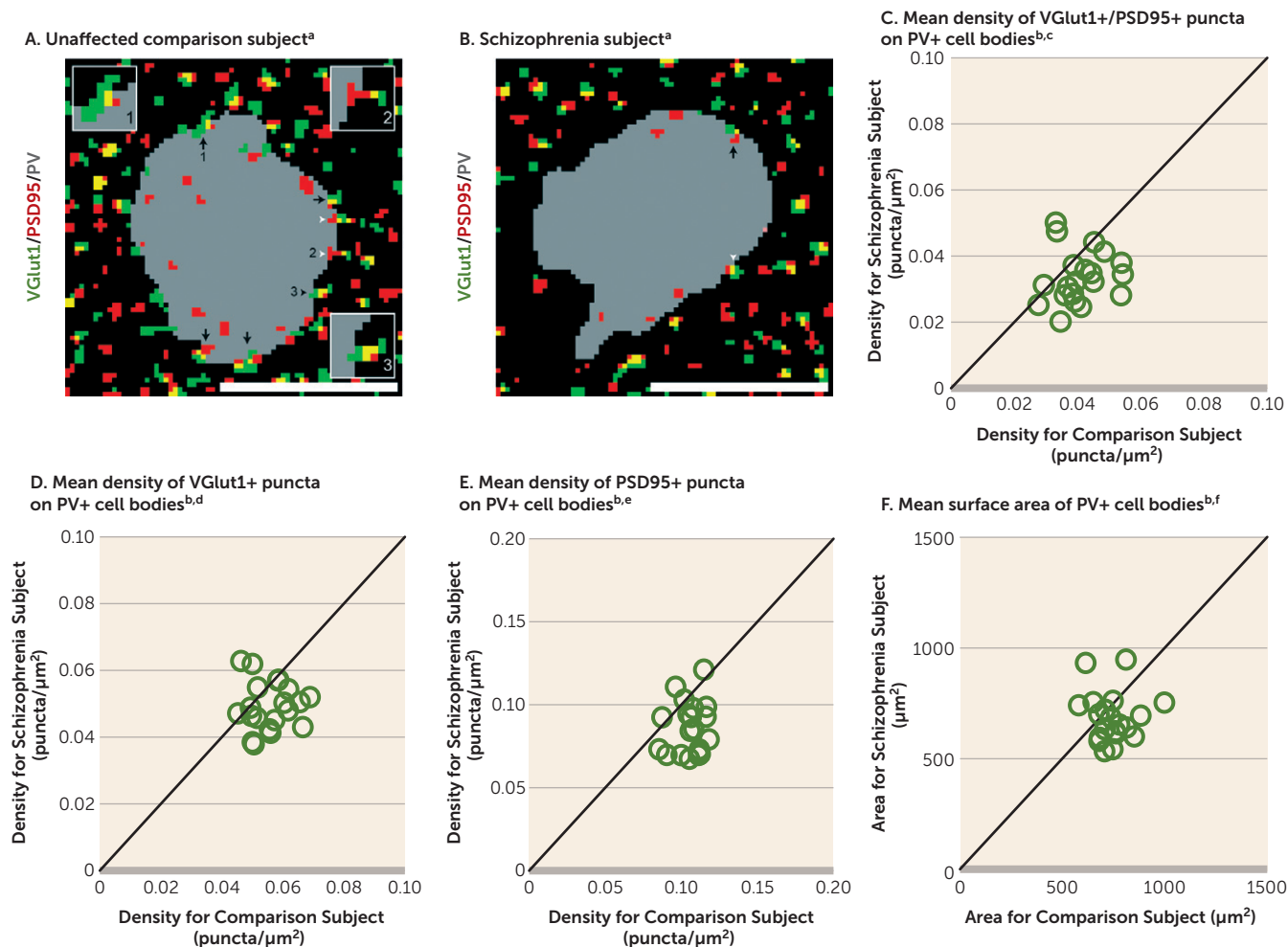
In order to determine the cell type specificity of the lower number of excitatory synapses on PV+ neurons, we measured the density of excitatory synapses on CR+ neurons. The mean numbers of sampled CR+ neurons, mean somal CR protein

levels, and mean surface area of CR+ cell bodies did not differ between subject groups (Figures 3A–C). The mean density of VGlut1+/PSD95+ puncta on CR+ cell bodies was 9% higher in the schizophrenia subjects (Figure 3D), demonstrating that the number of excitatory synapses on CR+ neurons is not lower in the illness.

### Validation of Methods for Quantifying Excitatory Synaptic Inputs

We have previously shown by dual-labeling electron microscopy that the density of excitatory synapses is significantly higher (1.90-fold) on PV+ than CR+ neurons in the primate DLPFC (35). Consistent with these findings, the mean density of VGlut1+/PSD95+ puncta on PV+ cell bodies was significantly (1.73-fold) higher than on CR+ cell bodies in the comparison subjects in the present study (t=8.5, df=19, p<0.001). This finding indicates that the light microscopic

**FIGURE 2. Lower Density of Excitatory Synapses on PV+ Neurons in Schizophrenia Subjects Relative to Matched Unaffected Comparison Subjects**



<sup>a</sup> Panels A and B illustrate representative masked images of VGlut1+ puncta (green), PSD95+ puncta (red), and PV+ cell bodies (gray) from the subject pair shown in Figures 1A and 1B. Excitatory synapses on PV+ neurons were identified by the overlap of VGlut1+/PSD95+ puncta (yellow) within a PV+ cell body (black arrows, inset image 1). Overlapping VGlut1+/PSD95+ puncta (white arrowheads, inset image 2) or VGlut1+ puncta (black arrowheads, inset image 3) were located within a PV+ cell body were not included as excitatory synapses. Scale bars=10  $\mu\text{m}$ .

<sup>b</sup> In panels C–F, the scatterplots indicate the levels of dependent measures (indicated in the heading of each graph) for each unaffected comparison and schizophrenia subject in a pair. Data points below the diagonal unity line indicate a lower level in the schizophrenia subject relative to the matched unaffected comparison subject. Graphs C–E indicate significantly lower densities in the schizophrenia subjects than in the unaffected comparison subjects, as specified in the following footnotes.

<sup>c</sup> The mean density of VGlut1+/PSD95+ puncta was 18% lower in the schizophrenia subjects (mean=0.0335, SD=0.008) than in the comparison subjects (mean=0.0409, SD=0.008). The difference was statistically significant (paired:  $F=10.3$ ,  $df=1, 19$ ,  $p=0.005$ ; unpaired:  $F=11.4$ ,  $df=1, 36$ ,  $p=0.002$ ).

<sup>d</sup> The mean density of VGlut1+ puncta was 12% lower in the schizophrenia subjects (mean=0.0492, SD=0.007) than in the comparison subjects (mean=0.0558, SD=0.007). The difference was statistically significant (paired:  $F=8.9$ ,  $df=1, 19$ ,  $p=0.008$ ; unpaired:  $F=11.1$ ,  $df=1, 36$ ,  $p=0.002$ ).

<sup>e</sup> The mean density of PSD95+ puncta was 19% lower in the schizophrenia subjects (mean=0.0857, SD=0.016) than in the comparison subjects (mean=0.106, SD=0.010). The difference was statistically significant (paired:  $F=26.5$ ,  $df=1, 19$ ,  $p<0.001$ ; unpaired:  $F=34.7$ ,  $df=1, 35$ ,  $p<0.001$ ).

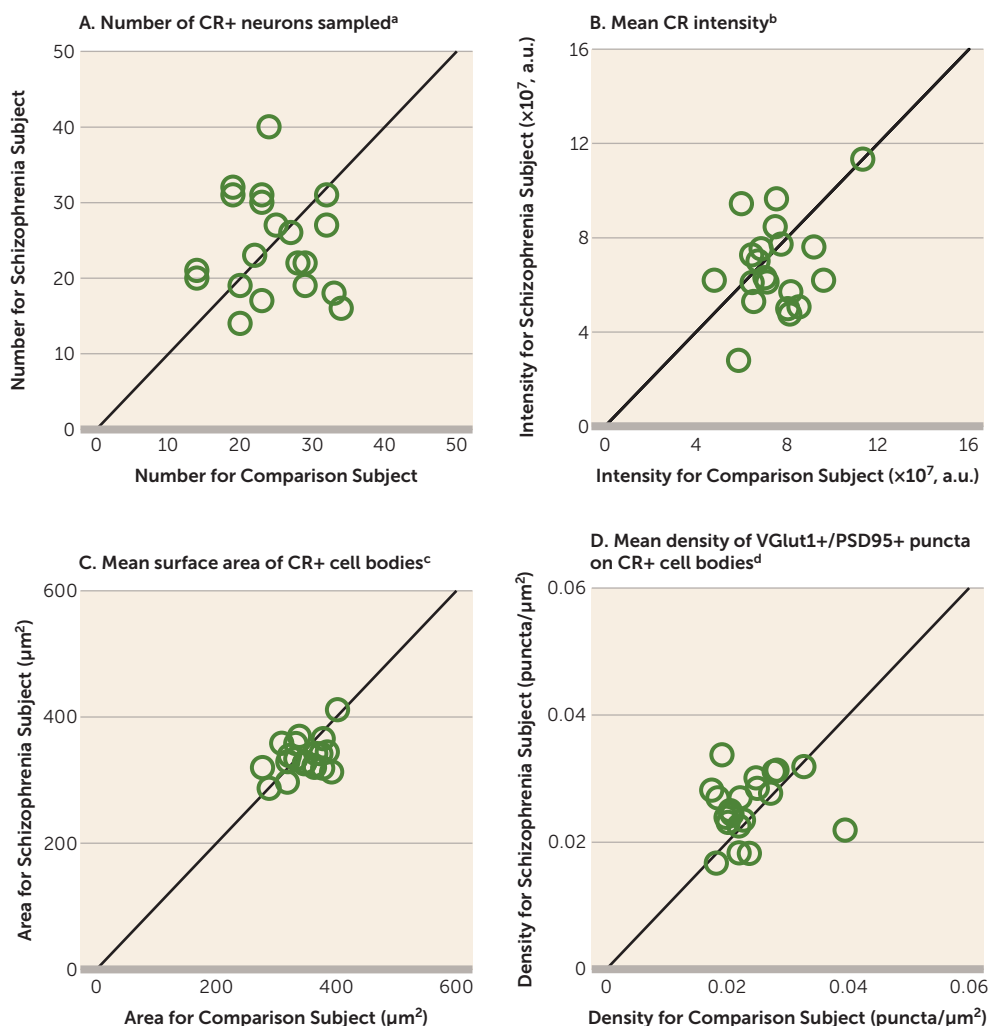
<sup>f</sup> The mean surface area of PV+ cell bodies was 8% lower in the schizophrenia subjects (mean=684, SD=111) than in the comparison subjects (mean=745, SD=96) but did not differ significantly between groups (paired:  $F=3.3$ ,  $df=1, 19$ ,  $p=0.09$ ; unpaired:  $F=3.5$ ,  $df=1, 36$ ,  $p=0.07$ ).

methods used here provide a robust means for sampling excitatory synaptic inputs specific to PV+ or CR+ neurons.

### Prediction of PV and GAD67 Expression in Human DLPFC by Excitatory Synapses on PV Interneurons

Finally, we assessed whether the density of excitatory synapses on PV+ neurons predicted levels of PV and GAD67, molecular markers of PV interneuron activity. Mean density of VGlut1+/PSD95+ puncta on PV+ cell bodies was positively

correlated with PV and GAD67 mRNA levels in schizophrenia subjects but not in comparison subjects (Figures 4A and 4B). In addition, the mean density of VGlut1+/PSD95+ puncta on PV+ cell bodies positively predicted the mean somal PV immunoreactivity levels in schizophrenia subjects but not in comparison subjects (Figure 4C). Moreover, this positive correlation was evident across all sampled PV+ neurons in both subject groups (Figure 4D). Among these neurons, the PV+ neurons with the lowest PV levels (more

**FIGURE 3. Quantification of Excitatory Synapses on CR+ Neurons in Dorsolateral Prefrontal Cortex Area 9 for Each Matched Pair of Unaffected Comparison and Schizophrenia Subjects**

<sup>a</sup> The mean number of sampled CR+ neurons was 0.8% lower in the schizophrenia subjects (mean=24.3, SD=6.7) than in the comparison subjects (mean=24.5, SD=5.9) but did not differ significantly between groups (paired:  $F=0.01$ ,  $df=1, 19$ ,  $p=0.93$ ; unpaired:  $F=0.01$ ,  $df=1, 36$ ,  $p=0.93$ ).

<sup>b</sup> The mean CR immunoreactivity level in CR+ cell bodies was 10% lower in the schizophrenia subjects (mean= $6.8 \times 10^7$ , SD= $2.0 \times 10^7$ ) than in the comparison subjects (mean= $7.5 \times 10^7$ , SD= $1.5 \times 10^7$ ) but did not differ significantly between groups (paired:  $F=2.6$ ,  $df=1, 19$ ,  $p=0.13$ ; unpaired:  $F=1.9$ ,  $df=1, 36$ ,  $p=0.19$ ). a.u., arbitrary units.

<sup>c</sup> The surface area of CR+ cell bodies was 3% lower in the schizophrenia subjects (mean=336, SD=28) than in the comparison subjects (mean=347, SD=34) but did not differ significantly between groups (paired:  $F=1.1$ ,  $df=1, 18$ ,  $p=0.32$ ; unpaired:  $F=1.7$ ,  $df=1, 36$ ,  $p=0.20$ ).

<sup>d</sup> The density of VGlut1+/PSD95+ puncta on CR+ cell bodies was 9% higher in the schizophrenia subjects (mean=0.0257, SD=0.005) than in the comparison subjects (mean=0.0236, SD=0.005). The difference was significant in the paired test ( $F=5.1$ ,  $df=1, 18$ ,  $p=0.04$ ) but not the unpaired test ( $F=1.5$ ,  $df=1, 36$ ,  $p=0.24$ ).

than one standard deviation below the mean) had a density of VGlut1+/PSD95+ puncta 42% lower than the PV+ neurons with the highest PV levels (more than one standard deviation above the mean), and the difference was statistically significant ( $t=-5.4$ ,  $df=112$ ,  $p<0.001$ ).

## DISCUSSION

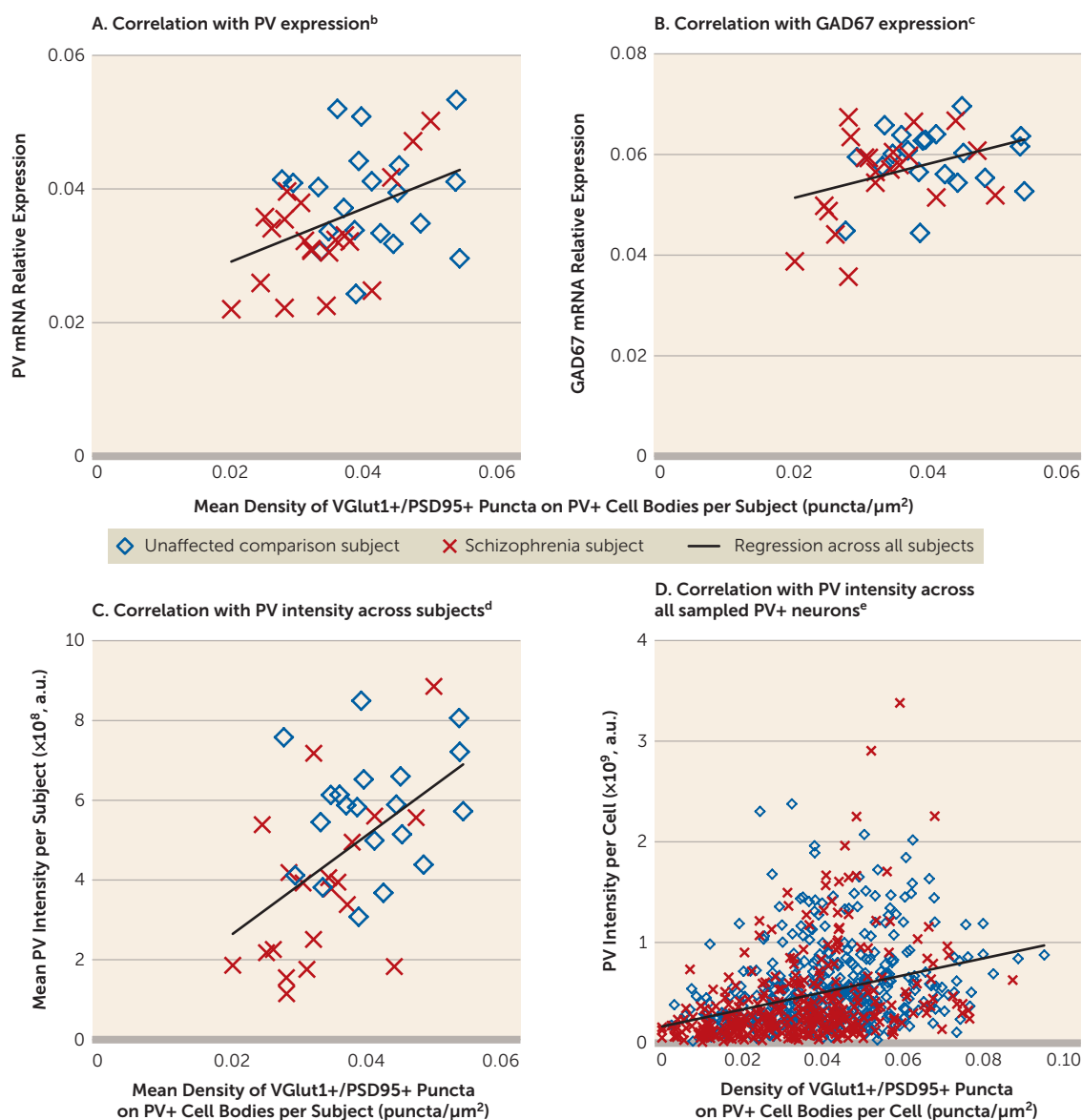
A pathological substrate for reduced glutamatergic drive onto PV interneurons in schizophrenia has not been previously

identified due to the technical challenges of resolving synaptic abnormalities in a cell type-specific manner in post-mortem human brain. Here we report for the first time, to our knowledge, that the neuropathology of schizophrenia includes a lower number of excitatory synapses on PV interneurons. This deficit appears to reflect the disease process of schizophrenia and is not due to methodological confounds or other factors commonly associated with the illness. First, the presence of fewer excitatory synapses on PV+ neurons was evident from lower numbers of both pre- and postsynaptic markers, validating deficits in the synaptic structures. Second, these deficits were not confounded by either a larger surface area of PV+ cell bodies or undetectable levels of protein markers within existing synaptic structures in schizophrenia subjects. Third, none of the assessed schizophrenia-associated comorbid factors accounted for these deficits. Fourth, long-term exposure to antipsychotic medications did not alter the density of excitatory synapses on PV+ neurons in the DLPFC of nonhuman primates; the effect of antipsychotics could not be assessed in humans, as only one schizophrenia subject had not been exposed to these medications. Fifth, the density of excitatory synapses on CR+ neurons was not lower

in the illness, consistent with a prominent pathology of PV interneurons in schizophrenia. Finally, the density of excitatory synapses on PV+ neurons predicted levels of the activity-dependent gene products PV and GAD67 selectively in the schizophrenia subjects. Together, these findings support the hypothesis that fewer excitatory synapses selectively on cortical PV interneurons provide a pathological substrate for deficient excitatory drive to these interneurons in schizophrenia.

PV interneurons comprise two main subtypes: PV basket neurons target the proximal dendrites and cell bodies of

**FIGURE 4. Association Between Density of Excitatory Synapses on PV+ Neurons and Activity-Dependent Expression Levels of PV and GAD67 Selectively in Schizophrenia Subjects<sup>a</sup>**



<sup>a</sup> a.u., arbitrary units.

<sup>b</sup> The mean density of VGlut1+/PSD95+ puncta on PV+ cell bodies positively predicted the relative mRNA levels of PV in the schizophrenia subjects but not in the comparison subjects (all subjects:  $r=0.43$ ,  $p=0.007$ ; comparison subjects:  $r=0.03$ ,  $p=0.90$ ; schizophrenia subjects:  $r=0.59$ ,  $p=0.006$ ).

<sup>c</sup> The mean density of VGlut1+/PSD95+ puncta on PV+ cell bodies positively predicted the relative mRNA levels of GAD67 in the schizophrenia subjects but not in the comparison subjects (all subjects:  $r=0.37$ ,  $p=0.02$ ; comparison subjects:  $r=0.15$ ,  $p=0.54$ ; schizophrenia subjects:  $r=0.44$ ,  $p=0.053$ ).

<sup>d</sup> Across subjects, the mean density of VGlut1+/PSD95+ puncta on PV+ cell bodies positively predicted the mean somal PV immunoreactivity level in the schizophrenia subjects but not in the comparison subjects (all subjects:  $r=0.53$ ,  $p<0.001$ ; comparison subjects:  $r=0.20$ ,  $p=0.41$ ; schizophrenia subjects:  $r=0.56$ ,  $p=0.02$ ).

<sup>e</sup> Across all sampled PV+ neurons ( $N=725$ ), the density of VGlut1+/PSD95+ puncta on PV+ cell bodies positively predicted somal PV immunoreactivity levels in both groups (all subjects:  $r=0.33$ ,  $p<0.001$ ; comparison subjects:  $r=0.26$ ,  $p<0.001$ ; schizophrenia subjects:  $r=0.34$ ,  $p<0.001$ ).

pyramidal neurons, and PV chandelier neurons synapse onto the axon initial segment of pyramidal neurons (36). Although both populations of PV interneuron subtypes are active during gamma oscillations, gamma rhythms are more strongly coupled to the activity of PV basket neurons (37, 38). Given the much greater prevalence of PV basket neurons in the middle layers of the primate DLPFC (39, 40), most of the PV+ neurons sampled in our study are likely to be PV basket neurons.

Our sampling of excitatory synapses on PV+ neurons is limited in two respects. First, we did not sample VGlut2-containing excitatory inputs that represent projections from the thalamus (41). However, thalamic axons represent a small minority (<10%) of excitatory terminals in the cortex (42), and only a small percentage of thalamic inputs target PV interneurons (43), suggesting that the excitation of PV interneurons is mostly driven by cortical excitatory inputs.

Second, we did not sample synaptic inputs to dendrites of PV interneurons due to the few dendrites with detectable PV immunoreactivity that originate from PV+ cell bodies. Although the density of excitatory synapses is higher on dendrites than cell bodies of PV interneurons (44), depolarization of the cell body of PV interneurons is much stronger for somal than dendritic excitatory inputs (45, 46). However, despite these limitations, the density of excitatory cortical synapses on PV+ cell bodies in the present study predicted activity-dependent PV expression across all PV+ neurons. Therefore, our approach was sufficiently sensitive to detect an apparently functionally meaningful deficit in excitatory synaptic inputs to PV+ neurons in schizophrenia subjects.

Multiple signaling pathways regulate the formation of excitatory synapses on PV interneurons. For example, the ErbB4 signaling pathway induces the formation of excitatory synapses on PV interneurons (11, 47, 48), and the release of neuronal pentraxin 2 (Narp) from pyramidal cells recruits excitatory synapses selectively on PV interneurons in an activity-dependent manner (28). Both an abnormal shift in ErbB4 splicing at the JM locus (49, 50) and lower Narp transcript levels have been shown in the DLPFC of subjects with schizophrenia, including those included in the present study (21, 51). Across these subjects, the density of VGlut1+/PSD95+ puncta on PV+ cell bodies was significantly correlated with the ratio of ErbB4 JM-a to JM-b splice variants in cortical layer 4 ( $r = -0.44$ ,  $p = 0.005$ ) and with Narp mRNA levels in total gray matter ( $r = 0.35$ ,  $p = 0.03$ ). These findings suggest that alterations in the ErbB4 and/or Narp signaling pathways could be upstream of the deficit in excitatory synaptic inputs to, and consequently the lower activity of, PV interneurons in schizophrenia.

Consistent with the idea that PV interneuron activity is reduced in the illness, activity-dependent expression levels of GAD67 are lower in the DLPFC of subjects with schizophrenia, and specifically in PV interneurons (15, 17). Experimental reductions of GAD67 in PV interneurons decrease inhibitory synaptic transmission in pyramidal cells and alter cortical network activity (52–54). Strong inhibition of pyramidal cells by PV interneurons is required for the generation of gamma oscillations in the DLPFC associated with working memory. Thus, the lower density of excitatory synapses on PV+ neurons and the corresponding deficit in GAD67 expression found in the present study could provide a pathological substrate for deficient inhibition of pyramidal cells by PV interneurons, which in turn would result in impaired gamma oscillations and working memory deficits in people with schizophrenia.

Discovering pathological entities that bridge etiopathogenic pathways to the core features of the illness is essential for understanding the disease process of schizophrenia. For example, disruptions in the ErbB4 or Narp signaling pathway in the DLPFC could be upstream of the deficits in excitatory synaptic inputs to PV interneurons in schizophrenia. Given that PV interneuron activity is essential for gamma oscillations, these deficits could underlie the downstream pathophysiology of impaired gamma oscillations and consequently working

memory dysfunction in schizophrenia. Therefore, fewer excitatory synapses on PV interneurons might serve as a common pathological locus upon which diverse streams of etiopathogenic pathways converge in order to produce a core pathophysiological feature of schizophrenia from which cognitive dysfunction emerges.

## AUTHOR AND ARTICLE INFORMATION

From the Translational Neuroscience Program, Department of Psychiatry, and the Medical Scientist Training Program, University of Pittsburgh School of Medicine, Pittsburgh.

Address correspondence to Dr. Lewis (lewisda@upmc.edu).

Presented in part at the 15th International Congress on Schizophrenia Research, Colorado Springs, Colo., March 28 to April 1, 2015, and the 3rd Annual Molecular Psychiatry Meeting, San Francisco, Oct. 30 to Nov. 1, 2015.

Supported by NIMH grants MH043784 and MH103204 to Dr. Lewis and NIMH grant MH096985 to Dr. Fish.

The authors thank Kelly Rogers, M.S., and Mary Brady, B.S., of the University of Pittsburgh for technical assistance.

Dr. Lewis currently receives investigator-initiated research support from Pfizer and in 2013–2015 served as a consultant in the areas of target identification and validation and new compound development to Autifony, Bristol-Myers Squibb, Concert Pharmaceuticals, and Sunovion. The other authors report no financial relationships with commercial interests.

Received Jan. 6, 2016; revision received March 14, 2016; accepted April 8, 2016; published online July 22, 2016.

## REFERENCES

- Kahn RS, Keefe RS: Schizophrenia is a cognitive illness: time for a change in focus. *JAMA Psychiatry* 2013; 70:1107–1112
- Keefe RS, Harvey PD: Cognitive impairment in schizophrenia. *Handb Exp Pharmacol* 2012; 213:11–37
- Uhlhaas PJ, Singer W: Abnormal neural oscillations and synchrony in schizophrenia. *Nat Rev Neurosci* 2010; 11:100–113
- Sohal VS, Zhang F, Yizhar O, et al: Parvalbumin neurons and gamma rhythms enhance cortical circuit performance. *Nature* 2009; 459:698–702
- Cardin JA, Carlén M, Meletis K, et al: Driving fast-spiking cells induces gamma rhythm and controls sensory responses. *Nature* 2009; 459:663–667
- Coyle JT, Basu A, Benneyworth M, et al: Glutamatergic synaptic dysregulation in schizophrenia: therapeutic implications. *Handb Exp Pharmacol* 2012; 213:267–295
- Moghaddam B, Krystal JH: Capturing the angel in “angel dust”: twenty years of translational neuroscience studies of NMDA receptor antagonists in animals and humans. *Schizophr Bull* 2012; 38:942–949
- Gonzalez-Burgos G, Lewis DA: NMDA receptor hypofunction, parvalbumin-positive neurons, and cortical gamma oscillations in schizophrenia. *Schizophr Bull* 2012; 38:950–957
- Behrens MM, Ali SS, Dao DN, et al: Ketamine-induced loss of phenotype of fast-spiking interneurons is mediated by NADPH-oxidase. *Science* 2007; 318:1645–1647
- Belforte JE, Zsiros V, Sklar ER, et al: Postnatal NMDA receptor ablation in corticolimbic interneurons confers schizophrenia-like phenotypes. *Nat Neurosci* 2010; 13:76–83
- Del Pino I, García-Frigola C, Dehorter N, et al: ErbB4 deletion from fast-spiking interneurons causes schizophrenia-like phenotypes. *Neuron* 2013; 79:1152–1168
- Pelkey KA, Barksdale E, Craig MT, et al: Pentraxins coordinate excitatory synapse maturation and circuit integration of parvalbumin interneurons. *Neuron* 2015; 85:1257–1272
- Akbarian S, Kim JJ, Potkin SG, et al: Gene expression for glutamic acid decarboxylase is reduced without loss of neurons in prefrontal cortex of schizophrenics. *Arch Gen Psychiatry* 1995; 52:258–266

14. Volk DW, Austin MC, Pierri JN, et al: Decreased glutamic acid decarboxylase67 messenger RNA expression in a subset of prefrontal cortical gamma-aminobutyric acid neurons in subjects with schizophrenia. *Arch Gen Psychiatry* 2000; 57:237–245
15. Hashimoto T, Volk DW, Eggan SM, et al: Gene expression deficits in a subclass of GABA neurons in the prefrontal cortex of subjects with schizophrenia. *J Neurosci* 2003; 23:6315–6326
16. Fung SJ, Webster MJ, Sivagnanasundaram S, et al: Expression of interneuron markers in the dorsolateral prefrontal cortex of the developing human and in schizophrenia. *Am J Psychiatry* 2010; 167:1479–1488
17. Curley AA, Arion D, Volk DW, et al: Cortical deficits of glutamic acid decarboxylase 67 expression in schizophrenia: clinical, protein, and cell type-specific features. *Am J Psychiatry* 2011; 168:921–929
18. Woo TU, Miller JL, Lewis DA: Schizophrenia and the parvalbumin-containing class of cortical local circuit neurons. *Am J Psychiatry* 1997; 154:1013–1015
19. Enwright JF, Sanapala S, Foglio A, et al: Reduced labeling of parvalbumin neurons and perineuronal nets in the dorsolateral prefrontal cortex of subjects with schizophrenia. *Neuropsychopharmacology* (Epub ahead of print, Feb 12, 2016)
20. Condé F, Lund JS, Jacobowitz DM, et al: Local circuit neurons immunoreactive for calretinin, calbindin D-28k or parvalbumin in monkey prefrontal cortex: distribution and morphology. *J Comp Neurol* 1994; 341:95–116
21. Chung DW, Volk DW, Arion D, et al: Dysregulated ErbB4 splicing in schizophrenia: selective effects on parvalbumin expression. *Am J Psychiatry* 2016; 173:60–68
22. Porta EA: Pigments in aging: an overview. *Ann N Y Acad Sci* 2002; 959:57–65
23. Glausier JR, Fish KN, Lewis DA: Altered parvalbumin basket cell inputs in the dorsolateral prefrontal cortex of schizophrenia subjects. *Mol Psychiatry* 2014; 19:30–36
24. Sweet RA, Henteleff RA, Zhang W, et al: Reduced dendritic spine density in auditory cortex of subjects with schizophrenia. *Neuropsychopharmacology* 2009; 34:374–389
25. Pierri JN, Chaudry AS, Woo TU, et al: Alterations in chandelier neuron axon terminals in the prefrontal cortex of schizophrenic subjects. *Am J Psychiatry* 1999; 156:1709–1719
26. Gabbott PL, Jays PR, Bacon SJ: Calretinin neurons in human medial prefrontal cortex (areas 24a,b,c, 32', and 25). *J Comp Neurol* 1997; 381:389–410
27. Rocco BR, Lewis DA, Fish KN: Markedly lower glutamic acid decarboxylase 67 protein levels in a subset of boutons in schizophrenia. *Biol Psychiatry* (Epub ahead of print, Aug 7, 2015)
28. Chang MC, Park JM, Pelkey KA, et al: Narp regulates homeostatic scaling of excitatory synapses on parvalbumin-expressing interneurons. *Nat Neurosci* 2010; 13:1090–1097
29. Donato F, Rompani SB, Caroni P: Parvalbumin-expressing basket-cell network plasticity induced by experience regulates adult learning. *Nature* 2013; 504:272–276
30. Fish KN, Sweet RA, Deo AJ, et al: An automated segmentation methodology for quantifying immunoreactive puncta number and fluorescence intensity in tissue sections. *Brain Res* 2008; 1240:62–72
31. Canny J: A computational approach to edge detection. *IEEE Trans Pattern Anal Mach Intell* 1986; 8:679–698
32. Dorph-Petersen KA, Pierri JN, Perel JM, et al: The influence of chronic exposure to antipsychotic medications on brain size before and after tissue fixation: a comparison of haloperidol and olanzapine in macaque monkeys. *Neuropsychopharmacology* 2005; 30:1649–1661
33. Kimoto S, Bazmi HH, Lewis DA: Lower expression of glutamic acid decarboxylase 67 in the prefrontal cortex in schizophrenia: contribution of altered regulation by Zif268. *Am J Psychiatry* 2014; 171:969–978
34. Volk DW, Chitrapu A, Edelson JR, et al: Chemokine receptors and cortical interneuron dysfunction in schizophrenia. *Schizophr Res* 2015; 167:12–17
35. Melchitzky DS, Lewis DA: Pyramidal neuron local axon terminals in monkey prefrontal cortex: differential targeting of subclasses of GABA neurons. *Cereb Cortex* 2003; 13:452–460
36. Williams SM, Goldman-Rakic PS, Leranath C: The synaptology of parvalbumin-immunoreactive neurons in the primate prefrontal cortex. *J Comp Neurol* 1992; 320:353–369
37. Massi L, Lagler M, Hartwich K, et al: Temporal dynamics of parvalbumin-expressing axo-axonic and basket cells in the rat medial prefrontal cortex in vivo. *J Neurosci* 2012; 32:16496–16502
38. Dugladze T, Schmitz D, Whittington MA, et al: Segregation of axonal and somatic activity during fast network oscillations. *Science* 2012; 336:1458–1461
39. Krimer LS, Zaitsev AV, Czanner G, et al: Cluster analysis-based physiological classification and morphological properties of inhibitory neurons in layers 2-3 of monkey dorsolateral prefrontal cortex. *J Neurophysiol* 2005; 94:3009–3022
40. Zaitsev AV, Gonzalez-Burgos G, Povysheva NV, et al: Localization of calcium-binding proteins in physiologically and morphologically characterized interneurons of monkey dorsolateral prefrontal cortex. *Cereb Cortex* 2005; 15:1178–1186
41. Fremeau RT Jr, Troyer MD, Pahner I, et al: The expression of vesicular glutamate transporters defines two classes of excitatory synapse. *Neuron* 2001; 31:247–260
42. Latawiec D, Martin KA, Meskenaite V: Termination of the geniculocortical projection in the striate cortex of macaque monkey: a quantitative immunoelectron microscopic study. *J Comp Neurol* 2000; 419:306–319
43. Rotaru DC, Barrionuevo G, Sesack SR: Mediodorsal thalamic afferents to layer III of the rat prefrontal cortex: synaptic relationships to subclasses of interneurons. *J Comp Neurol* 2005; 490:220–238
44. Hioki H: Compartmental organization of synaptic inputs to parvalbumin-expressing GABAergic neurons in mouse primary somatosensory cortex. *Anat Sci Int* 2015; 90:7–21
45. Hu H, Martina M, Jonas P: Dendritic mechanisms underlying rapid synaptic activation of fast-spiking hippocampal interneurons. *Science* 2010; 327:52–58
46. Norenberg A, Hu H, Vida I, et al: Distinct nonuniform cable properties optimize rapid and efficient activation of fast-spiking GABAergic interneurons. *Proc Natl Acad Sci USA* 2010; 107:894–899
47. Ting AK, Chen Y, Wen L, et al: Neuregulin 1 promotes excitatory synapse development and function in GABAergic interneurons. *J Neurosci* 2011; 31:15–25
48. Mei L, Nave KA: Neuregulin-ERBB signaling in the nervous system and neuropsychiatric diseases. *Neuron* 2014; 83:27–49
49. Law AJ, Kleinman JE, Weinberger DR, et al: Disease-associated intronic variants in the ErbB4 gene are related to altered ErbB4 splice-variant expression in the brain in schizophrenia. *Hum Mol Genet* 2007; 16:129–141
50. Joshi D, Fullerton JM, Weickert CS: Elevated ErbB4 mRNA is related to interneuron deficit in prefrontal cortex in schizophrenia. *J Psychiatr Res* 2014; 53:125–132
51. Kimoto S, Zaki MM, Bazmi HH, et al: Altered markers of cortical  $\gamma$ -aminobutyric acid neuronal activity in schizophrenia: role of the NARP gene. *JAMA Psychiatry* 2015; 72:747–756
52. Lazarus MS, Krishnan K, Huang ZJ: GAD67 deficiency in parvalbumin interneurons produces deficits in inhibitory transmission and network disinhibition in mouse prefrontal cortex. *Cereb Cortex* 2015; 25:1290–1296
53. Brown JA, Ramikie TS, Schmidt MJ, et al: Inhibition of parvalbumin-expressing interneurons results in complex behavioral changes. *Mol Psychiatry* 2015; 20:1499–1507
54. Georgiev D, Yoshihara T, Kawabata R, et al: Cortical gene expression after a conditional knockout of 67 kDa glutamic acid decarboxylase in parvalbumin neurons. *Schizophr Bull* (Epub ahead of print, March 15, 2016)